Inorganic Chemistry
Article

Inorg. Chem. 2010, 49, 9247–9252 9247
DOI: 10.1021/ic100753g

Dynamic Changes in Dimensional Structures of Co-Complex Crystals

Atsushi Kondo,[†,‡,∥] Tomohiro Nakagawa,[‡] Hiroshi Kajiro,[*,§] Ayako Chinen,[‡] Yoshiyuki Hattori,[⊥] Fujio Okino,[⊥] Tomonori Ohba,[‡] Katsumi Kaneko,[‡,¶] and Hirofumi Kanoh[*,‡]

[†]*Collaborative Innovation Center for Nanotech FIBER (nanoFIC), Shinshu University, Ueda Nagano 386-8567, Japan,* [‡]*Graduate School of Science, Chiba University, Yayoi, Inage, Chiba 263-8522, Japan,* [§]*Nippon Steel Corporation, Shintomi, Futtsu, Chiba 293-8511, Japan, and* [⊥]*Department of Chemistry, Faculty of Textile Science and Technology, Shinshu University, Ueda 386-8567, Japan.* [∥]*Present address: Department of Applied Chemistry, Tokyo University of Agriculture and Technology, 2-24-16 Naka-cho, Koganei, Tokyo 184-8588, Japan.* [¶]*Present address: Institute of Carbon Science & Technology, Shinshu University, Wakasato 4-17-1, Nagano, 380-8553, Japan.*

Received April 20, 2010

A two-dimensional flexible porous coordination polymer (2D-PCP) that shows expansion/shrinkage structural transformation accompanied by molecular accommodation was synthesized by control of dimensionality in zero-dimensional and one-dimensional PCPs: The dynamic structural transformation cooperatively proceeds in the solid state with a drastic molecular rearrangement. Kinetics of the structural transformation was investigated.

Introduction

Crystal solids that involve the coordination of organic ligands to metal ions, in particular porous coordination polymers (PCPs) and metal−organic frameworks (MOFs), have received much attention because of their unique physical and chemical properties.[1,2] Their specific functionalities are highly dependent on the framework structures, and to this day, obtaining target compounds with the desired dimensional and/or geometrical frameworks remains a difficult challenge. In general, the synthesis of MOFs is carried out in solution, and many factors such as the temperature, pH, type of solvent, and concentration of solution influence the self-assembly process. If the means to control the dimension and/or the geometry of these compounds can be realized, there will be a large scope for research in applications such as gas storage, separation, sensors, catalysis, and optics.

A solid system provides a good example for understanding the build-up of crystal units because the decrease of the influential factors is expected compared with the solution system. Furthermore, direct observation of the process is possible. In fact, structural transformations in solid state have been observed experimentally.[3] A discrete complex is the coordination compound with the lowest dimensionality, and it can be considered as the core of coordination polymers.[4] We found that a discrete complex could undergo a drastic crystal phase transformation to form complexes with higher order frameworks (1D or 2D) (Scheme 1). According to the X-ray diffraction (XRD) results, a nonporous discrete complex crystal can be transformed to a nonporous 1D crystal and subsequently to a highly flexible

*To whom correspondence should be addressed. E-mail: kanoh@pchem2.s.chiba-u.ac.jp (H. Kanoh), kajiro.hiroshi@nsc.co.jp (H. Kajiro).

(1) (a) Hagrman, P. J.; Hagrman, D.; Zubieta, J. *Angew. Chem.* **1999**, *111*, 2798–2848. Hagrman, P. J.; Hagrman, D.; Zubieta, J. *Angew. Chem., Int. Ed.* **1999**, *38*, 2638−2684. (b) Moulton, B.; Zawarotko, M. *J. Chem. Rev.* **2001**, *101*, 1629–1658. (c) Khlobystov, A. N.; Blake, A. J.; Champness, N. R.; Lemenovskii, D. A.; Majouga, A. G.; Zyk, N. V.; Schröder, M. *Coord. Chem. Rev.* **2001**, *222*, 155–192. (d) Carlucci, L.; Ciani, G.; Proserpio, D. M. *Coord. Chem. Rev.* **2003**, *246*, 247–289. (e) Janiak, C. *Dalton Trans.* **2003**, 2781–2804. (f) Yaghi, O. M.; O'Keeffe, M.; Ockwig, N. W.; Chae, H. K.; Eddaoudi, M.; Kim, J. *Nature* **2003**, *423*, 705–714. (g) Kitagawa, S.; Kitaura, R.; Noro, S. *Angew. Chem.* **2004**, *116*, 2388–2430. Kitagawa, S.; Kitaura, R.; Noro, S. *Angew. Chem., Int. Ed.* **2004**, *43*, 2334−2375. (h) Férey, G. *Chem. Soc. Rev.* **2008**, *37*, 191–214. (i) Noro, S.; Kitagawa, S.; Akutagawa, T.; Nakamura, T. *Prog. Polym. Sci.* **2009**, *34*, 240–279.

(2) (a) Lee, S. J.; Hupp, J. T. *Coord. Chem. Rev.* **2006**, *250*, 1710–1723. (b) Dincă, M.; Long, J. R. *Angew. Chem.* **2008**, *130*, 6870–6884. Dincă, M.; Long, J. R. *Angew. Chem., Int. Ed.* **2008**, *47*, 6766−6779. (c) Shimomura, S.; Horike, S.; Matsuda, R.; Kitagawa, S. *J. Am. Chem. Soc.* **2007**, *129*, 10990–10991. (d) Kitagawa, S.; Matsuda, R. *Coord. Chem. Rev.* **2007**, *251*, 2490–2509. (e) Ghosh, S. K.; Kaneko, W.; Kiriya, D.; Ohba, M.; Kitagawa, S. *Angew. Chem.* **2008**, *120*, 8975–8979. *Angew. Chem., Int. Ed.* **2008**, *47*, 8843-8847. (f) Serre, C.; Mellot-Draznieks, C.; Surblé, S.; Audebrand, N.; Filinchuk, Y.; Férey, G. *Science* **2007**, *315*, 1828–1831. (g) Kanoh, H.; Kondo, A.; Noguchi, H.; Kajiro, H.; Tohdoh, A.; Hattori, Y.; Xu, W.-C.; Inoue, M.; Sugiura, T.; Morita, K.; Tanaka, H.; Ohba, T.; Kaneko, K. *J. Colloid Interface Sci.* **2009**, *334*, 1–7. (h) Ma, S.; Sun, D.; Simmons, J. M.; Collier, C. D.; Yuan, D.; Zhou, H.-C. *J. Am. Chem. Soc.* **2008**, *130*, 1012–1016. (i) Zeng, M.-H.; Wang, Q.-X.; Tan, Y.-X.; Hu, S.; Zhao, H.-X.; Long, L.-S.; Kurmoo, M. *J. Am. Chem. Soc.* **2010**, *132*, 2561–2563.

(3) (a) Toda, F.; Tanaka, K.; Tamashima, T.; Kato, M. *Angew. Chem.* **1998**, *110*, 2852–2855. Toda, F.; Tanaka, K.; Tamashima, T.; Kato, M. *Angew. Chem., Int. Ed.* **1998**, *37*, 2724−2727. (b) Atwood, J. L.; Barbour, L. J.; Jerga, A.; Schottel, B. L. *Science* **2002**, *298*, 1000–1002. (c) Tanaka, T.; Tasaki, T.; Aoyama, Y. *J. Am. Chem. Soc.* **2002**, *124*, 12453–12462. (d) Matsuda, R.; Kitaura, R.; Kitagawa, S.; Kubota, Y.; Kobayashi, T. C.; Horike, S.; Takata, M. *J. Am. Chem. Soc.* **2004**, *126*, 14063–14070. (e) Fletcher, A. J.; Thomas, K. M.; Rosseinsky, M. J. *J. Solid State Chem.* **2005**, *178*, 2491–2510. (f) Vittal, J. J. *Coord. Chem. Rev.* **2007**, *251*, 1781–1795. (g) Zeng, M.-H.; Hu, S.; Chen, Q.; Xie, G.; Shuai, Q.; Gao, S.-L; Tang, L.-Y. *Inorg. Chem.* **2009**, *48*, 7070–7079.

Published on Web 09/15/2010

Scheme 1. Hierarchical Assembly of Discrete Complexes to Form Higher-Order Dimensional Complexes[a]

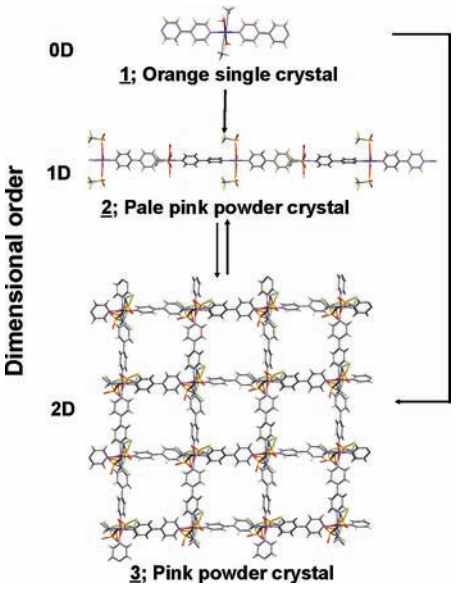

[a] Guest molecules are omitted for clarity.

microporous stacked-type 2D compound through polymerization involving the ligand substitution and drastic lattice reformation. The ability to control these dynamic structural transformations may open many avenues for synthesizing novel porous coordination polymers. In the present work, we describe the dynamic structural transformation of a discrete complex, $\{[Co(bpy)_2(CH_3CN)_2(H_2O)_2]\cdot 2(OTf)\}$ (**1**)[5a] (where bpy=4,4′-bipyridine, OTf=trifluoromethanesulfonate), into a 1D chain of the coordination polymer, $\{[Co(bpy)(OTf)_2(H_2O)_2]\cdot(bpy)\}$ (**2**),[5b] and then into a 2D square-grid sheet type of flexible PCP, $[Co(bpy)_2(OTf)_2]$ (**3**),[5c] that shows unique gas adsorption properties. In addition, we propose a mechanism for the cooperative substitution reaction and discuss the kinetics of the transformation.

Experimental Section

Reagent. Silver trifluoromethanesulfonate and cobalt(II) bromide were purchased from Sigma-Aldrich Co., Inc. Acetonitrile was purchased from Kanto Chemical Co., Inc. The ligand bpy was purchased from Tokyo Chemical Industry Co., Ltd. and recrystallized from methanol (2 times) and from CH_2Cl_2-hexane before use. Cobalt(II) trifluoromethanesulfonate was prepared in reference to the reported procedure using silver trifluoromethanesulfonate and cobalt(II) bromide.[6]

Synthesis of Compounds 1−3. For **1**, an acetonitrile solution of bpy (200 mM, 2.0 mL) was carefully layered onto an acetonitrile−water (15 vol% of water) mixed solution of $Co(OTf)_2$ (100 mM, 2.0 mL) after adding acetonitrile (1.0 mL) in a straight glass tube at room temperature. After a few days, orange single crystals were obtained. For **2**, **1** was filtrated and washed with acetonitrile and obtained crystals were exposed to atmosphere for 30 min to yield **2** as pale pink crystals. For **3**, multiroutes can be available. Crystal **2** was heated to 423 K for 2 h in a vacuum ($< 10^{-2}$ Pa) to yield **3**. In addition, **3** can be obtained by immersion of **1** into dehydrated acetonitrile for 10 days. Because **3** was highly moisture sensitive, **3** was treated under nitrogen atmosphere during IR measurement.

Data Collection and X-ray Structural Analyses. Data were collected on a Bruker SMART CCD area detector diffractometer (Mo Kα radiation λ = 0.71073 Å) at 173 K for **1** by the ω scan method. Empirical absorption corrections (SADABS) were applied in all cases. The structure was solved by direct methods (SIR97) and refined by full-matrix least-squares on F^2 (SHELX-97). Anisotropic thermal factors were assigned to all non-hydrogen atoms.

Synchrotron X-ray powder diffraction (XRPD) patterns of **2** and **3** were collected at BL02B2 SPring-8 with a large Debye−Scherrer Camera[7] (λ = 1.002 Å) at room temperature. The powder sample was loaded into a glass capillary with 0.3-mm outer diameter for the measurements. The cell parameters of **2** and **3** were determined by indexing program *n*-TREOR[8] and DICVOL91,[9] respectively. For **2**, the structural solution was performed on the EXPO2004 software[10] with the direct method. For **3**, an initial structure was based on an analogue single crystal structure. The cell parameters, peak shift parameters, profile parameters, and structural parameters were refined by Rietveld analysis using RIETAN software.[11] The peak shape was modeled by a pseudo-Voigt function.

XRPD Pattern Measurements through the Dynamic Structural Change between 1 and 2. XRPD measurements were performed on an improved Bruker MXP3 system with graphite-monochromated Cu Kα radiation (λ = 1.5406 Å) by a fixed time method operated at 1000 W power (40 kV, 25 mA) (Figure 3S, Supporting Information).

Temperature-Programmed Desorption (TPD) Mass Analyses, Thermal Gravimetric (TG) Analyses, and IR Measurements. The TPD-mass measurements of **1** and **2** were conducted on a laboratory designed TPD-mass system in the temperature range from 323 to 473 K with a heating rate of 3 K/min under He flow

(4) (a) Ranford, J. D.; Vittal, J. J.; Wu, D. *Angew. Chem.* **1998**, *110*, 1159–1162. Ranford, J. D.; Vittal, J. J.; Wu, D. *Angew. Chem., Int. Ed.* **1998**, *37*, 1114−1116. (b) Chu, Q.; Swenson, D. C.; MacGillivray, L. R. *Angew. Chem.* **2005**, *117*, 3635–3638. Chu, Q.; Swenson, D. C.; MacGillivray, L. R. *Angew. Chem., Int. Ed.* **2005**, *44*, 3569−3572. (c) Sudik, A. C.; Côté, A. P.; Wong-Foy, A. G.; O'Keeffe, M.; Yaghi, O. M. *Angew. Chem.* **2006**, *118*, 2590–2595. Sudik, A. C.; Côté, A. P.; Wong-Foy, A. G.; O'Keeffe, M.; Yaghi, O. M. *Angew. Chem., Int. Ed.* **2006**, *45*, 2528−2533. (d) Liu, Y.; Eubank, J. F.; Cairns, A. J.; Eckert, J.; Kravtsov, V. C.; Luebke, R.; Eddaoudi, M. *Angew. Chem.* **2007**, *119*, 3342–3347. Liu, Y.; Eubank, J. F.; Cairns, A. J.; Eckert, J.; Kravtsov, V. C.; Luebke, R. *Angew. Chem., Int. Ed.* **2007**, *46*, 3278−3283. (e) Kondo, A.; Noguchi, H.; Kajiro, H.; Ohba, T.; Kaneko, K.; Kanoh, H. *Langmuir* **2008**, *24*, 170–174.

(5) (a) Crystal data for **1**: $C_{26}H_{26}CoF_6N_6O_8S_2$, M = 787.58, triclinic, $P\bar{1}$ (No. 1), a = 7.0365(10), b = 10.5029(15), c = 12.1466(17) Å, α = 72.090(2), β = 86.029(2), γ = 77.182(2)°, V = 832.9(2) Å^3, Z = 1, ρ_{calcd} = 1.570 g cm^{-3}, $\mu(Mo_{K\alpha})$ = 0.729 mm^{-1}, θ_{max} = 28.44° ($-8 \le h \le 9$, $-12 \le k \le 12$, $-16 \le l \le 12$), T = 298 K, 3421 reflections out of 4210 unique reflections with $I > 2\sigma(I)$, goodness of fit = 1.028, final R factors R_1 = 0.0380, wR_2 = 0.0943. (b) Crystal data for **2**: $C_{22}H_{20}CoF_6N_4O_8S_2$, M = 705.49, orthorhombic, $Pccn$ (No. 56), a = 7.854(5), b = 15.051(5), c = 22.974(5) Å, V = 2715.77 Å^3, Z = 4, ρ_{calcd} = 1.726 g cm^{-3}, room temperature, R_p = 0.0242, R_{wp} = 0.0351. (c) Kondo, A.; Chinen, A.; Kajiro, H.; Nakagawa, T.; Kato, K.; Takata, M.; Hattori, Y.; Okino, F.; Ohba, T.; Kaneko, K.; Kanoh, H. *Chem.—Eur. J.* **2009**, *31*, 7549−7553. Crystal data for 3: $C_{22}H_{16}CoF_6N_4O_6S_2$, M = 669.46, Monoclinic, $C2c$ (No. 15), a = 25.8872(17), b = 15.309(5), c = 16.8265(11) Å, β = 111.219(1)°, V = 6216.37 Å^3, Z = 8, ρ_{calcd} = 1.431 g cm^{-3}, room temperature, R_p = 0.0409, R_{wp} = 0.0637. CCDC-745069 (**1**), CCDC-745067 (**2**), and CCDC-745068 (**3**) contain the supplementary crystallographic data for this paper. These data can be obtained free of charge from the Cambridge Crystallographic Data Centre via www.ccdc. cam.ac.uk/data_request/cif.

(6) Arduini, A. L.; Garnett, M.; Thompson, R. C.; Womg, T. C. T. *Can. J. Chem.* **1975**, *53*, 3812–3819.

(7) Nishibori, E.; Takata, M.; Kato, K.; Sakata, M.; Kubota, Y.; Aoyagi, S.; Kuroiwa, Y.; Yamakata, M.; Ikeda, N. *Nucl. Instr. Meth. Phys. Res. A* **2001**, *467−468*, 1045–1048.

(8) Altomare, A.; Giacovazzo, C.; Guagliardi, A.; Moliterni, A. G. G.; Rizzi, R.; Werner, P.-E. *J. Appl. Crystallogr.* **2000**, *33*, 1180–1186.

(9) Boultif, A.; Louër, D. *J. Appl. Crystallogr.* **1991**, *24*, 987–993.

(10) Altomare, A.; Burla, M. C.; Camalli, M.; Carrozzini, B.; Cascarano, G. L.; Giacovazzo, C.; Guagliardi, A.; Moliterni, A. G. G.; Polidori, G.; Rizzi, R. *J. Appl. Crystallogr.* **1999**, *32*, 339–340.

(11) Izumi, F.; Ikeda, T. *Mater. Sci. Forum* **2000**, *198*, 321–324.

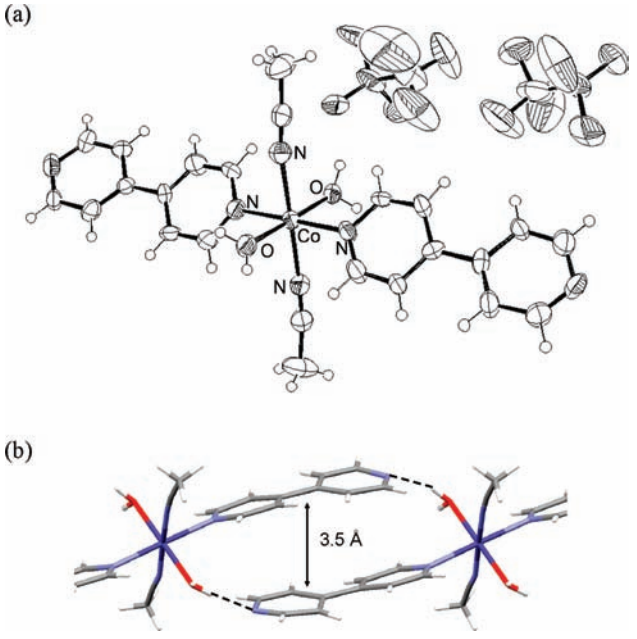

Figure 1. Crystal structure of **1**. (a) ORTEP representation of the asymmetric unit of **1** with 50% probability. (b) Connection between the discrete units. C: gray, Co: dark blue, H: white, N: light blue, O: red. Hydrogen bondings are shown as dashed black lines in (b).

to examine the removal process of molecules (Figures 1S and 5S, Supporting Information).

TG measurements of **1** and **2** were performed on a Seiko Instruments Inc. TG-DTA6200 under nitrogen gas flow (150 mL/min) (Figures 2S and 6S, Supporting Information). Samples were heated from room temperature to 873 K, at a heating rate of 3 K/min.

IR spectra of **1**, **2**, and **3** were measured at room temperature using a Perkin-Elmer FT-IR System 2000 spectrometer with ATR attachment (DurasamplIR, Sensir Technologies Co., Inc.) under nitrogen atmosphere. The summation was four consecutive scans and the resolution was 4 cm^{-1}. IR of **1** (cm^{-1}): 3367, 2942, 2281, 2253, 1610, 1559, 1539, 1495, 1418, 1376, 1244, 1222, 1157, 1069, 1029, 1011, 920, 861, 818, 757, 733, 633. **2** (cm^{-1}): 3366, 1609, 1536, 1493, 1416, 1284, 1238, 1215, 1157, 1067, 1024, 858, 810, 761, 732, 675, 631. **3** (cm^{-1}): 3082, 1611, 1539, 1495, 1419, 1312, 1236, 1211, 1160, 1069, 1026, 862, 819, 805, 761, 732, 675, 631. IR spectra of **1** and **3** were measured to check the presence/absence of water molecules at room temperature using an in situ IR cell with CaF_2 windows with the aid of an FT-IR spectrometer JASCO FT-IR-550 (Figure 9S, Supporting Information). The IR spectra were measured with the summation of 1024 consecutive scans and a resolution of 2 cm^{-1}.

Adsorption Measurements and Analyses. The adsorption isotherms of N_2 at 77 K were carried out by a volumetric automatic equipment (Quantachrome, Autosorb-1). Nitrogen gas of high purity (>99.9999%) was used. Prior to the sorption isotherm measurements, the samples were outgassed under a vacuum ($<10^{-2}$ Pa) at 423 K for 2 h.

Results and Discussion

The reaction in wet acetonitrile solution of $Co(OTf)_2$ and bpy with a metal/ligand ratio of 1/2 at ambient temperature produces the orange-colored block-shaped single crystals of **1**. Structural analysis by single-crystal XRD at 298 K revealed that **1** is a discrete complex in which the Co(II) ion is surrounded by two bpy, two CH_3CN, and two H_2O molecules, forming a slightly distorted octahedral coordination geometry (Figure 1a). The discrete units connect via $\pi-\pi$ interaction of bpy (centroid−plane separation 3.5 Å) and hydrogen bondings between the N atoms of bpy molecules and the H atoms of H_2O molecules (N···H 1.91 and 1.93 Å), forming quasi-1D chains aligned in parallel along the *c* axis (Figures 1b and 11S). The interchain gap is 9.99 Å wide and is filled with guest molecules of the OTf anions (Figure 11S, Supporting Information). The OTf anions connect the quasi-1D chains by the hydrogen bondings between the O atoms of OTf anions and the H atoms of water molecules (O···H 1.9−2.1 Å) and by the weak interactions between the O atoms of OTf anions and the H atoms of bpy ligands (O···H 2.6−2.7 Å) and between the O atoms of OTf anions and the H atoms of acetonitrile molecules (O···H 2.5−2.8 Å). Owing to the prevention of OTf anions, there is no calculated accessible void volume and **1** is nonporous.[12]

When left in atmospheric conditions, **1** lost the coordinated acetonitrile molecules, resulting in a drastic structural rearrangement of the building blocks, and transforms to **2** (Figures 2 and 12S). XRD analysis showed that the resultant **2** has a 1D chain comprising Co(II) ions and bpy ligands in which the distance between metal centers is 11.49 Å. The Co(II) ion is in octahedral coordination with two N atoms from bpy, two O atoms from water, and two O atoms from OTf anions. There are two distinct bpy molecules in **2**: one is directly coordinated to Co(II) ions to form the 1D chains and the other is a guest molecule connecting the 1D chains with the hydrogen bondings between the N atoms of bpy and the H atoms of water molecules (N···H 2.0 Å, N···O 2.8 Å), thereby forming quasi-2D rectangular shaped frameworks (11.49 × 15.05 $Å^2$, Figure 2a). The quasi-2D sheets stack along the *a* axis in an ABAB fashion with offsets of *b*/2 and almost ∼*c*/4 (0.26 *c* or 0.24 *c*), as shown in Figure 2b. In this configuration, the metal centers are positioned close to the center of the adjacent rectangular grid. Since the rectangular grid sheets are closely stacked (3.9 Å), there is no calculated open void in **2**.[12]

This drastic rearrangement requires the breaking of coordination bondings between Co(II) ions and bpy ligands, and of hydrogen bondings between N atoms of bpy and H atoms of coordinated water molecules. The coordination sites occupied by the acetonitrile molecules are replaced by OTf anions that must move by 3.3 Å (Figure 3a).[13] Furthermore, hydrogen-bonded bpy ligands must rotate to form the new bihydrogen-bonded structure. The $\pi-\pi$ interaction between bpy molecules facilitates this dynamic rotation. Interestingly, these dynamic structural changes cannot occur in a vacuum, suggesting an important role for moisture in air (Figure 3S, Supporting Information). In fact, the presence of additional water molecules explains the drastic rearrangement confirmed by in situ XRD experiments (Figure 4).

When **2** was heated to 423 K for 2 h in a vacuum, a further dynamic structural change was observed. XRD analysis showed that the coordinated water molecules were removed,[13,14] followed by the direct coordination of bpy molecules to Co(II) ions, yielding **3** with a 2D square-grid

(12) Spek, A. L. *PLATON, A Multipurpose Crystallographic Tool*; Utrecht University: Utrecht, The Netherlands, 2001.

(13) Bradshaw, D.; Warren, J. E.; Rosseinsky, M. J. *Science* **2007**, *315*, 977–980.

(14) (a) Kondo, A.; Noguchi, H.; Ohnishi, S.; Kajiro, H.; Tohdoh, A.; Hattori, Y.; Xu, W.-C.; Tanaka, H.; Kanoh, H.; Kaneko, K. *Nano Lett.* **2006**, *6*, 2581–2584. (b) Cheng, Y.; Kondo, A.; Noguchi, H.; Kajiro, H.; Urita, K.; Ohba, T.; Kaneko, K.; Kanoh, H. *Langmuir* **2009**, *25*, 4510–4513.

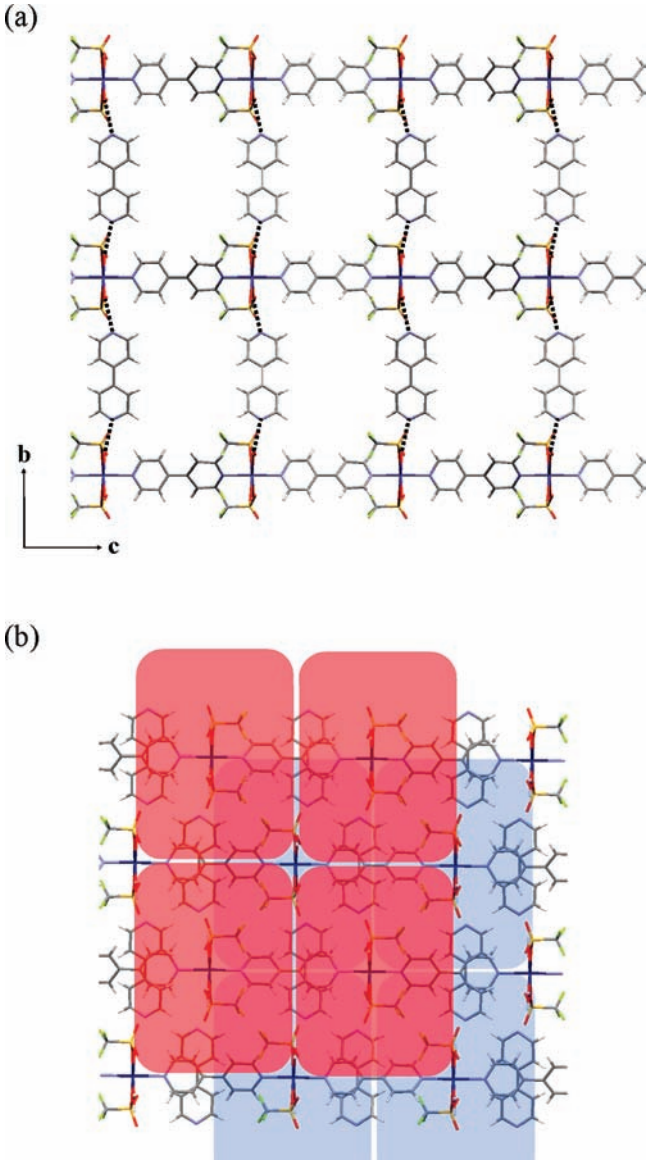

Figure 2. (a) A schematic representation of one quasi-2D rectangular layer in **2**, in which the size of the rectangle is 11.49 × 15.05 Å^2 and (b) stacking mode of the 2D layers. The hydrogen bondings are shown in dotted black lines in (a).

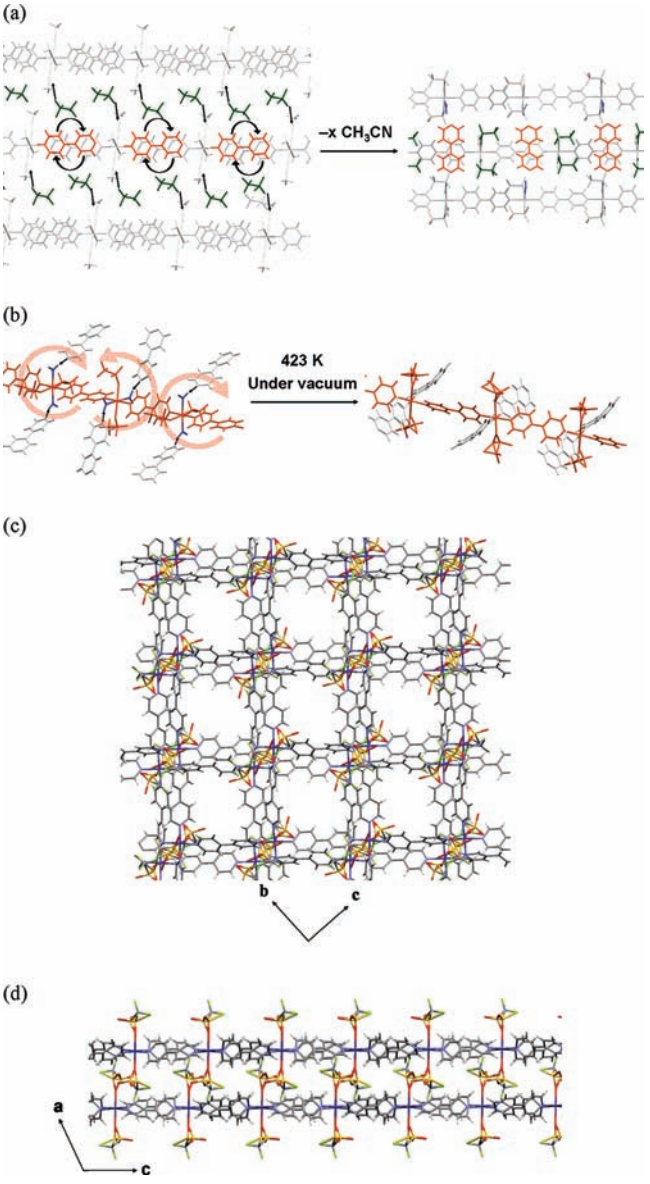

Figure 3. (a) Proposed mechanism for the dynamic structural rearrangement from **1** (0D) to **2** (1D). The anions, OTf anions, and one kind of bpy molecules are shown in green and orange, respectively. (b) Dynamic structural rearrangement of **2** (1D) to **3** (2D) by removal of coordinated water molecules (blue color). Schematic representations of **3** (c) along *a* and (d) *b* axis, respectively.

stacked structure (Figures 3b−3d and 13S).[5c] The 2D square-grid sheets stack along the *a* axis in an ABAB fashion with sheet separations of 6.5 and 5.6 Å. Weak interlayer interactions were observed between O atoms of OTf anions and H atoms of bpy ligands over long distances (O···H 2.5−2.9 Å). The substitution reaction was accompanied by a rotation of the Co coordination sphere and by the decrease in distance between 1D arrays (Co···Co distance: from 15.05 Å in **2** to 11.37 Å in **3**) that allowed the bidentate guest bpy molecules to bind the 1D arrays. Through this reaction, the unit cell volume was increased by 14.8% because of the increase in interlayer distance. The material also changed from being nonporous to being open microporous with a pore volume of 0.13 mL/g.[12] The framework structure of **3** is almost the same as that of a previously investigated PCP, and the crystal has unique gas adsorption properties.[5c]

Crystal **3** could also be obtained by heating **1** to 423 K for 2 h in a vacuum ($< 10^{-1}$ Pa). TG and TPD-mass analysis showed that **1** releases water and acetonitrile molecules at 423 K (Figures 1S and 2S). Therefore, heat-treated **1** should have a molecular ratio Co/bpy/OTf of 1:2:2. The XRD patterns, and hence the structures, of the heat-treated **1** and **3** are very similar. When **3**, obtained either from **1** or **2**, was placed in atmospheric conditions, **2** was obtained as a result of water molecules being incorporated into the crystal. This indicates that the phase of **2** is the most stable form among **1**, **2**, and **3** under atmospheric conditions.

Crystal **3** showed the unique gas adsorption properties. The N_2 adsorption isotherm of **3** from **1** at 77 K is shown in Figure 5 with clear double steps in the adsorption branch and large hysteresis.[5c,15] As we reported before, the initial uptake

(15) Kondo, A.; Noguchi, H.; Carlucci, L.; Proserpio, D. M.; Ciani, G.; Kajiro, H.; Ohba, T.; Kanoh, H.; Kaneko, K. *J. Am. Chem. Soc.* **2007**, *129*, 12362–12363.

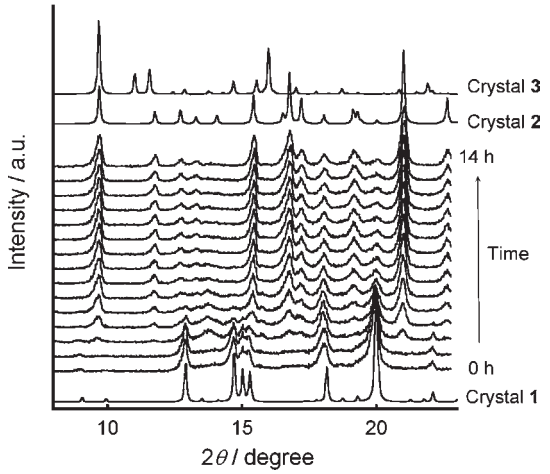

Figure 4. Time dependence of the XRPD pattern during the transformation from **1** to **2** at 293 K in 1.1 kPa water vapor over a time range of 14 h with an interval of 1 h with the simulated XRD patterns of **1**, **2**, and **3** (λ = 1.5406 Å).

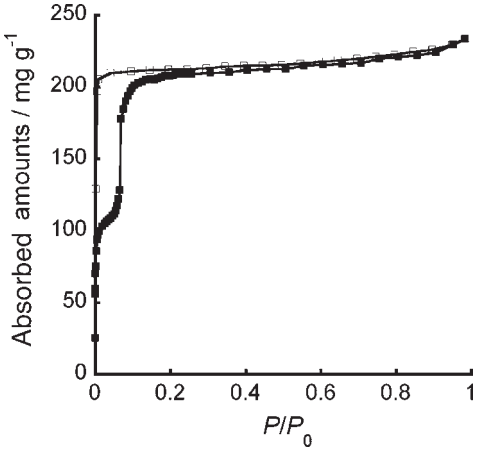

Figure 5. Nitrogen adsorption (filled squares) and desorption (open squares) isotherms of **3** at 77 K.

is due to the micropore filling in the inherent micropores, and the second to the expansive modulation of the 2D layered PCP.[5c,14a,15,16] The pore parameters are also similar to those of the 2D PCP we previously reported.[5c] To the best of our knowledge, this is the first novel case for synthesizing the flexible 2D layered PCP, with unique gas adsorption characteristics, from a discrete complex.

Of the structural changes described above, the most striking one is that from **1** to **2**, arising from the large displacement of OTf anions and the rotation of bpy molecules by about 90°, leading to the drastic framework rearrangement. The kinetics of this transformation was investigated. Figure 6 shows the time evolution of the XRD pattern from **1** to **2,** after the introduction of water vapor of 1.1 kPa. The peaks assigned to **1** (0D) gradually decreased in intensity with the growth of the peaks assigned to **2** (1D). Some of the main peaks were selected and integrated to measure the average

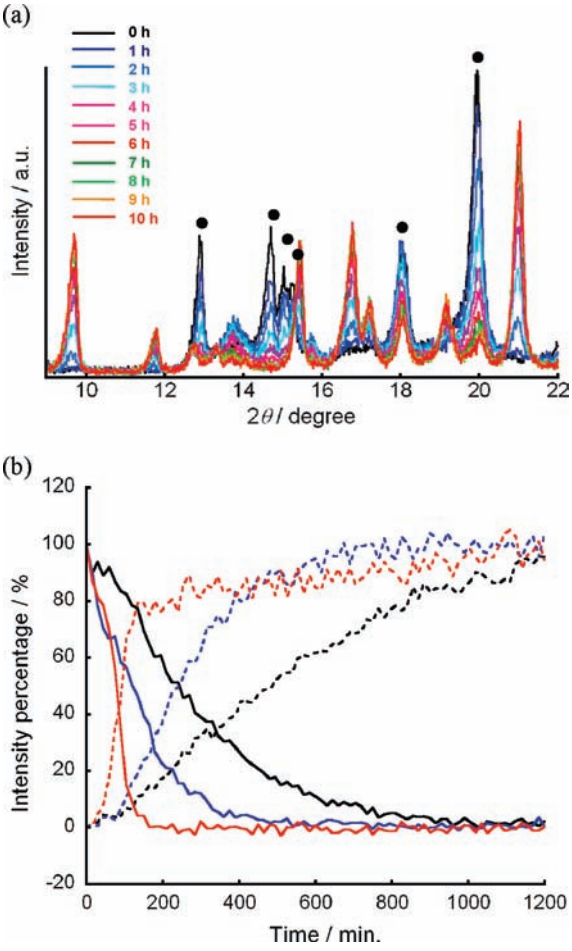

Figure 6. (a) Time evolution of the XRD pattern during the transformation from **1** to **2** at 293 K in 1.1 kPa water vapor over a time range of 10 h (λ = 1.5406 Å). The dotted peaks (●) are assigned to **1**. (b) Time courses of averaged intensities of the 0D (solid lines) and 1D crystal (dotted lines) in 1.1 kPa water vapor, calculated from selected XRD peaks for different temperatures. The black, blue, and red are at 291, 293, and 298 K, respectively.

Table 1. Formation and Decomposition Rate Constants for the Structural Change between **1** and **2** at 291 to 298 K in 1.1 kPa Water Vapor

rate constant	291 K	293 K	298 K
k_F /10^{-4} s^{-1}	1.0	1.8	4.7
k_D /10^{-4} s^{-1}	0.71	1.4	6.5

relative intensities as functions of time for several temperatures (Figure 6b).[17] The results clearly showed that structural transformations occur faster at higher temperatures. At lower temperature, the retention time was observed before structural transformation especially in the formation process of **2** (1D). The induction time, which depends on the temperature, is required for nucleation before the formation of the 1D crystal. The decomposition rates (k_D) of the 0D compound and the formation rates (k_F) of the 1D structure were estimated assuming a first-order reaction (Table 1). The rates of decomposition and formation are relatively slow (10^{-5} to 10^{-4} s^{-1}) under these conditions.

(16) (a) Noguchi, H.; Kondoh, A.; Hattori, Y.; Kanoh, H.; Kajiro, H.; Kaneko, K. *J. Phys. Chem. B* **2005**, *109*, 13851–13853. (b) Noguchi, H.; Kondo, A.; Hattori, Y.; Kajiro, H.; Kanoh, H.; Kaneko, K. *Adsorpt. Sci. Technol.* **2006**, *24*, 595–600. (c) Noguchi, H.; Kondo, A.; Hattori, Y.; Kajiro, H.; Kanoh, H.; Kaneko, K. *J. Phys. Chem. C* **2007**, *111*, 248–254.

(17) The peaks assigned to crystal **1** gradually decrease in intensity with the growth of the peaks assigned to crystal **2**. For the analysis, several main peaks (12.87, 14.69, 15.03, 15.21, 18.09, and 20.00 (2θ/deg) for crystal **1** and 9.71, 11.79, 15.47, 16.77, and 21.03 (2θ/deg) for crystal **2**) were selected.

The activation energy was estimated by the Arrhenius equation from reaction rates at different temperatures. The activation energies of decomposition (E_D) and formation (E_F) are 230 and 160 kJ/mol, respectively. The dynamic structural change from **3** to **2** was also investigated and similar trend was observed.

In conclusion, we showed the dynamic structural transformation of a discrete coordination compound to a 2D porous coordination polymer. The 2D compound indicated unique gas adsorption isotherms arising from the flexible expansion/shrinkage of the layers that facilitates the accommodation of gas molecules. We proposed a cooperative mechanism for the transformation by ligand substitution. In addition, the kinetics and energetics of the transformation were investigated. The series of dynamic hierarchical rearrangements show the possibility to synthesize new porous materials and provide hints for the dimensional and geometrical control of coordination compounds.

Acknowledgment. The synchrotron radiation experiments were performed at SPring-8 with the approval of the Japan Synchrotron Radiation Research Institute (JASRI) as a Nanotechnology Support Project of the Ministry of Education, Culture, Sports, Science and Technology (Proposal No. 2006A1587/BL02B2). This work was supported by a Grant-in-Aid for Fundamental Scientific Research (B) (No. 19350100) and projects for the "Innovation Creative Center for Advanced Interdisciplinary Research Areas (Shinshu University)" in Special Coordination Funds for Promoting Science and Technology from the Ministry of Education, Culture, Sports, Science, and Technology, Japan.

Supporting Information Available: Details of experimental procedures, structural information, and physical properties. This material is available free of charge via the Internet at http://pubs.acs.org.